Journal of Ovonic Research Vol. 4, No. 2, April 2008, p. 20 - 34

OPTICAL CONSTANTS OF THE THERMALLY EVAPORATED a-$Se_{70}Ge_{30}$ THIN FILMS

E. G. El-Metwally[a], M. O. Abou-Helal[b], I. S. Yahia[a*]
[a]*Semiconductor Lab., Physics Department, Faculty of Education, Ain Shams University, Roxy, Cairo, Egypt.*
[b]*Solid State Physics Dep., National Research Centre, El-Tahrir St., Dokki, Cairo, Egypt.*

Thermal evaporation technique was used to prepare a-$Ge_{70}Se_{30}$ thin films onto glass substrates of thicknesses range (108–717 nm). Transmittance measurements in the wavelength range (400-2500nm) were used to calculate the refractive index n and the extinction coefficient k using Swanepole's method. The calculated parameters such as optical band gap E_g^{opt}, the width of the tail of localized states in the band gap E_e, optical conductivity σ_{opt}, complex dielectric constant, relaxation time τ and dissipation factor $\tan\delta$ were determined. The analysis of the optical absorption data revealed that the optical band gap E_g^{opt} was indirect transitions. The optical dispersion parameters E_o and E_d were determined according to Wemple - DiDomenico method.

(Received March 18, 2008; accepted March 21, 2008)

Keywords: Amorphous semiconductor, Thin film, SeGe, Optical dispersion parameters, Dielectric constant, Dissipation factor, relaxation time, Optical conductivity.

1. Introduction

Chalcogenide glasses have recently drawn attention from scientists because of their potential use in various solid state devices [1,2,3]. Besides, the physical properties of chalcogenide semiconducting glasses are strongly dependent on their compositions [4,5]. Chalcogenide semiconductors have truly emerged as multipurpose materials and have been used to fabricate technological important devices: IR detector, electronic and optical switches and optical recording media [6]. Chalcogenide glasses of $Se_{70}Ge_{30}$ alloys are very interesting materials for infrared optics. They have a large range of transparency from around 0.6 to 30 mm and good mechanical and chemical properties, such as hardness, adhesion, low internal stress and water resistance. Optical properties of the $Se_{70}Ge_{30}$ system were reported by many authors [7,8]. This paper aims to investigate the optical constants of $Se_{70}Ge_{30}$ thin films deposited on glass substrates held at room temperature such as refractive index n, extinction coefficient k, optical band gap E_g^{opt}, the width of the tail of localized states in the band gap E_e, optical dispersion parameters E_o and E_d, complex dielectric constant, relaxation time τ, dissipation factor $\tan\delta$ and optical conductivity σ_{opt}.

*Corresponding author: dr_isyahia@yahoo.com

2. Experimental

$Se_{70}Ge_{30}$ was prepared by the usual melt quenching technique. The constituent elements Se (99.9%) and Ge (99.999%) were weighed and mixed in the appropriate stoichiometric proportion and sealed in evacuated (10^{-5} Torr) silica ampoule. The ampoule was placed in furnace and heated stepwise to 1223K to allow the elements to react completely. The ampoules were then kept at 1373K for about 15 h and shaken frequently to ensure that the melt was homogeneous. The ampoules are quenched in ice water from the melt state [9]. Thin films were prepared by thermal evaporation at 10^{-5}Torr using an Edwards coating system E-306. Molybdenum boats were used for evaporation. The thickness of the film was measured using a quartz crystal monitor Edward model FTMS. The structure of the investigated thin films shows the absence of any sharp diffraction lines, indicating that the amorphous nature of the investigated $Se_{70}Ge_{30}$ thin films [9]. The transmittance $T(\lambda)$ of the investigated sample films were measured in the spectral range (400–2500 nm) using SPECTROMETER/DATA SYSTEM, JASCO Corp., V- 570, Rev.1.00, for the as-deposited $Se_{70}Ge_{30}$ thin films for different thicknesses.

3. Results and discussion

3.1. Optical properties of $Se_{70}Ge_{30}$ thin films.

3.1.A. Method of calculation

The optical constants (refractive index n, extinction coefficient k, absorption coefficient α, and the optical energy gap E_g^{opt}) were determined using Swanepoel's method [10-13]. A thin film on a transp-arent substrate is shown in Fig.1. In this figure, d, n, α and T denote the film thickness, the refractive index, the absorption coefficient and the transmission, respectively. The transparent substrate has a thickness several orders of magnitude larger than d and has refractive index n_s and absorption coefficient $\alpha_s = 0$. The refractive index for air is taken to be $n_o = 1$. The transmission spectrum can roughly be divided into four regions [10,11]:

(i) In the transparent region, ($\alpha = 0$), the transmission is determined by n and n_s through multiple reflections.
(ii) In the region of weak absorption, α is small and transmission begins to decrease.
(iii) In the medium absorption, α is large, the transmission decreases mainly due to the effect of α.
(iv) In the region of strong absorption, the transmission decreases drastically due almost exclusively to the influence of α.

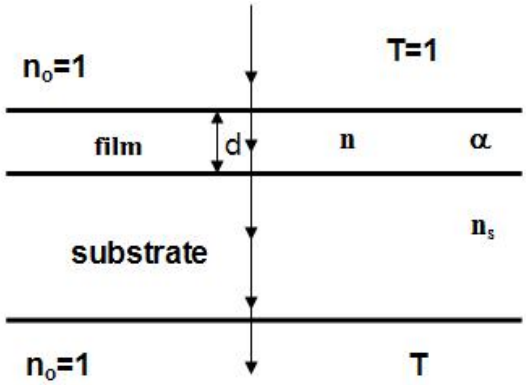

Fig.1 System of an absorbing thin film on a thick finite transparent substrate.

If the thickness d is uniform, interference effects give rise to the spectrum showed a maxima and minima of the transmission curve. These interference fringes can be used to calculate the optical constants of the film. The basic equations for the four regions are as follows [10-13]:
(i) For the transparent region the refractive index n is given by [13]:

$$n = \left[M + \left(M^2 - n_s^2\right)^{1/2}\right]^{1/2}, \tag{1}$$

where

$$M = \frac{2n_s}{T_{min}} - \frac{n_s^2+1}{2}, \tag{2}$$

(ii,iii) The region of weak and medium absorption, the refractive index n is given by [13]:-

$$n = \left[N + \left(N^2 - n_s^2\right)^{1/2}\right]^{1/2}, \tag{3}$$

where,

$$N = 2n_s \frac{T_{max} - T_{min}}{T_{max}T_{min}} + \frac{n_s^2+1}{2}, \tag{4}$$

For the absorption index k, the absorbance, x, is given in terms of the interference extremes using the following relation [13]:-

$$X = \frac{E_M - \left[E_M^2 - (n^2-1)^3(n^2-n_s^4)\right]^{1/2}}{(n-1)^3(n-n_s^2)}, \tag{5}$$

where,

$$E_m = \frac{8n^2n_s}{T_{max}} + (n^2-1)(n^2-n_s^2), \tag{6}$$

and

$$x = \exp(-4\pi kt/\lambda), \tag{7}$$

(iv) For the region of strong absorption where the interference maxima and minima converge to a single curve T_o, the absorbance, x, is given by [13]:-

$$x \cong T_o \frac{(n+1)^3(n+n_s^2)}{16n^2n_s}, \tag{8}$$

3.1.B. Determination of absorption coefficient α and optical energy gap E_g^{opt}.

The study of the optical absorption of the investigated amorphous $Se_{70}Ge_{30}$, particularly the absorption edge has proved to be very useful for elucidation of the electronic structure of these materials. The spectral distribution of the refractive index *n*, the extinction coefficient *k* and the

absorption coefficient α were determined using Swanepole's method [10]. In this section, we study the transmittance of the as deposited $Se_{70}Ge_{30}$ thin films. The analysis of the absorption coefficient has been carried out to obtain the optical energy gap E_g^{opt} and also, the analysis of the refractive index n with the help of the absorption index k has been carried out to obtain the real and imaginary part of complex dielectric constants (ε_1 , ε_2), dissipation factor $\tan\delta$, relaxation time τ and the optical conductivity σ_{opt}.

3.1.B.I. Spectral distribution of the transmittance as a function of wavelength

The spectral distribution of transmittance $T(\lambda)$ was studied for $Se_{70}Ge_{30}$ in the thickness range (108-717nm) using unpolarized light at normal incidence in the wavelength range (400-2500 nm). The obtained spectral distribution curves $T(\lambda)$ is illustrated in Fig.2 for $Se_{70}Ge_{30}$ thin films of different thicknesses.

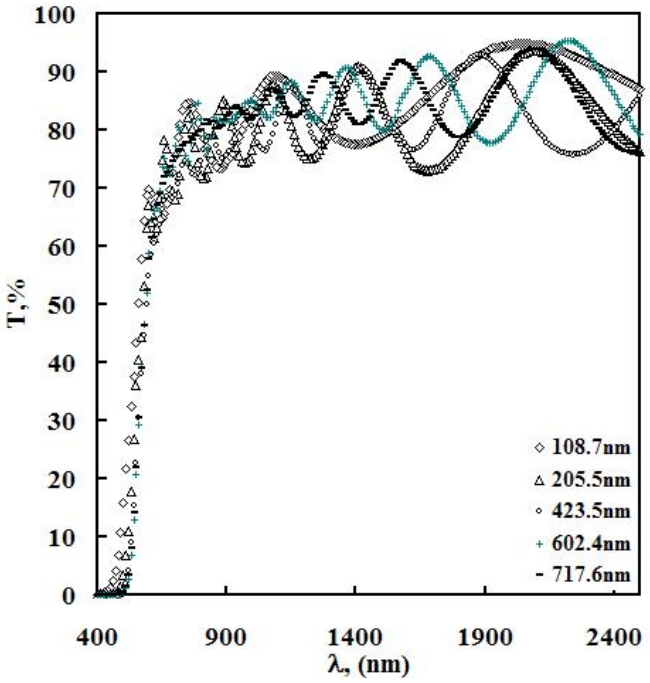

Fig. 2. Spectral distribution of the transmission $T(\lambda)$ for $Se_{70}Ge_{30}$ for different thin film thicknesses.

3.1.B.II. The refractive index n and absorption index k.

The refractive index n and absorption index k were computed from the obtained $T(\lambda)$ in the wavelength range (400-2500nm) using Swanepoel's method [10] for the investigated thicknesses. The spectral distributions of the mean values of n and k versus wavelength λ for the investigated thicknesses are shown in Figs.(3&4) respectively.

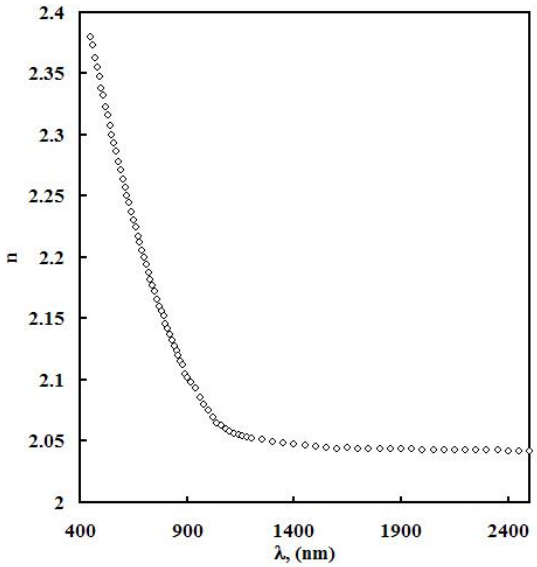

Fig.3 Dependence of the mean values of the refractive index n on the wavelength λ for the investigated sample thin films.

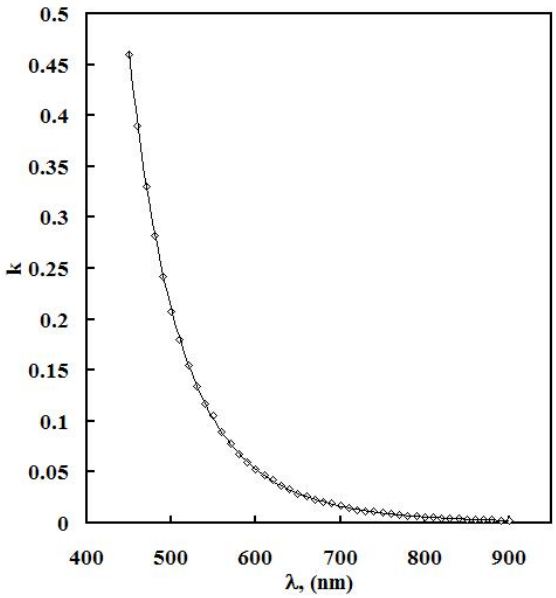

Fig.4 Dependence of the mean values of the extinction coefficient k on the wavelength λ for the investigated sample thin films.

3.1.B.III. Optical absorption edge.

The spectral distribution of the absorption coefficient α of the films was calculated from the relation $\alpha = 4\pi k / \lambda$, depend on the values of k calculated using Swanepoel's method. A plot of $\log \alpha$ as a function of photon energy $h\nu$ for $Se_{70}Ge_{30}$ thin film is illustrated in Fig.5. The optical absorption edge was analyzed by the following relation [14-16]:-

$$\alpha h\nu = A(h\nu - E_{g(1)}^{opt})^m, \qquad (9)$$

where A is the edge width parameter representing the film quality, which is calculated from the linear part of this relation, $E_{g(1)}^{opt}$ is the optical energy gap of the material and m determines the type of transition. The parameter m has the value *1/2* for the direct allowed transition and has the value *2* for the indirect allowed transition. The usual method for the determination of the value of $E_{g(1)}^{opt}$ involves a plotting of $(\alpha h\nu)^{1/2}$ and $(\alpha h\nu)^{2}$ against $h\nu$ as shown in Fig.6. This figure shows that $(\alpha h\nu)^{1/2}$ versus $h\nu$ is a linear function; this linearity indicates the existence of the allowed indirect transitions. The value of the energy gap $E_{g(1)}^{opt}$ is determined from the intercept of the extrapolation to zero absorption with the photon energy axis. Applying the least-square method to ensure the linearity behaviour of the obtained curves. Accordingly, values of the forbidden band gap $E_{g(1)}^{opt}$ and A were given in Table.1.

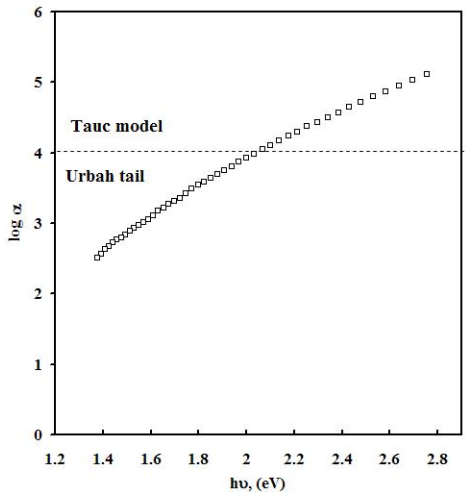

Fig.5 Dependence of the absorption coefficient $\log\alpha$ *on the photon energy* $h\nu$ *for the investigated sample thin films.*

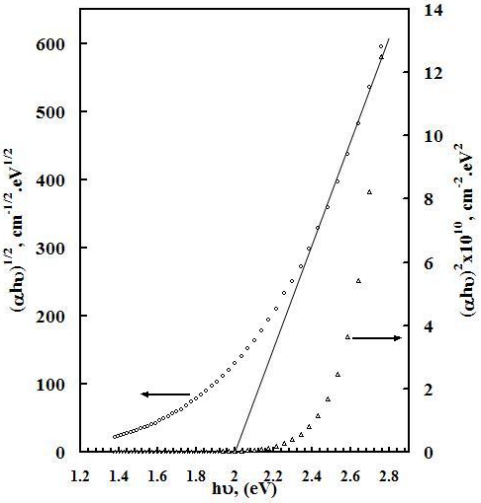

Fig.6. Dependence of $(\alpha h\nu)^{1/2}$ *and* $(\alpha h\nu)^{2}$ *on the photon energy* $h\nu$ *for the as-deposited thin films.*

The obtained results of $Se_{70}Ge_{30}$ thin films can be confirmed by plotting $h\nu\sqrt{\varepsilon_2}$ against $h\nu$ illustrated in Fig.7, where $\varepsilon_2 = 2nk$ (ε_2 is the imaginary part of the dielectric constant). The linear part of this graph, as described by the following relation [16-17]:

$$h^2\nu^2\varepsilon_2 \approx (h\nu - E_{g(2)}^{opt})^2 , \tag{10}$$

The extrapolation of this linear part yields $E_{g(2)}^{opt}$ indicates indirect optical transition for the investigated sample. The obtained values of the forbidden band gap $E_{g(2)}^{opt}$ from Fig.7 are in good agreement with those obtained from Fig. 6 for the investigated sample. The mean values of the forbidden band gap for $Se_{70}Ge_{30}$ equal 2±0.02eV. Values of $E_{g(2)}^{opt}$ was given in Table.1 for the investigated sample. The value of E_g^{opt} for indirect optical transition of $Se_{70}Ge_{30}$ films is in good agreement with those obtained before by N.A. Bakr [18], which equal 2eV for $Ge_{0.28}Se_{o.72}$ and 2.03 for $GeSe_3$ obtained by J. Reyes et al [19].

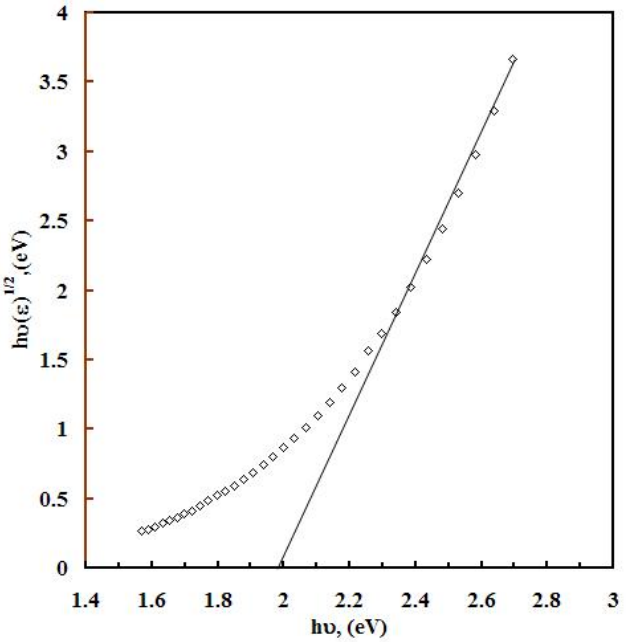

Fig. 7. Dependence of $h\nu(\varepsilon_2)^{1/2}$ *on the photon energy* $h\nu$ *for the investigated thin films.*

The second region of the absorption edge is for the lower values of the absorption coefficient, that is for α <l0^4 cm^{-1}, where the absorption at lower photon energy usually follows the Urbach rule [16] according to the following equation:

$$\alpha(\nu) = \alpha_o \exp(h\nu / E_e) , \tag{11}$$

where ν is the frequency of the radiation, α_o is a constant, h is Planck's constant and E_e is Urbach energy which is interpreted as the width of the tails of localized states in the band-gap and in general represents the degree of disorder in an amorphous semiconductor [16], the absorption in this region is due to transitions between extended states in one band and localized states in the

exponential tail of the other band. From plotting of $\log\alpha$ as a function of $h\nu$ as shown in Fig.5, it can be calculated the values of E_e and tabulated in Table 1.

Table 1. *Optical parameters of $Se_{70}Ge_{30}$ thin films.*

Material	**From Fig. 6** $E_{g(1)}^{opt}$ **, eV**	**From Fig. 7** $E_{g(2)}^{opt}$ **, eV**	A **,** $cm^{-1}.eV^{-1}$	E_e **, eV**
$Se_{70}Ge_{30}$	2.02	1.98	4.89×10^5	0.4537

3.1.B.IV. Dispersion energy parameters of $Se_{70}Ge_{30}$ thin films.

Wemple-DiDomenico [20-21] use a single-oscillator description of the frequency-dependent dielectric constant to define a "dispersion energy" parameters E_d and E_o. The refractive index dispersion of the sample studied can be fitted by the Wemple-DiDomenico. The dispersion plays an important role in the research for optical materials, because it is a significant factor in optical communication and in designing devices for spectral dispersion. Although these rules are quite different in detail, one common feature is the over-whelming evidence that both crystal structure and ionicity influence the refractive-index behaviour of solids in ways that can be simply described [21]. The relation between the refractive index n, and the single oscillator strength below the band gap is given by the expression [20-21]:

$$n^2 = 1 + \frac{E_o E_d}{E_o^2 - (h\nu)^2}\ , \tag{12}$$

where E_o and E_d are single oscillator constants, E_o is the energy of the effective dispersion oscillator, E_d the so-called dispersion energy, which measures the average strength of interband optical transitions. The oscillator energy E_o is an average of the optical band gap, E_g^{opt}, can be obtained from the Wemple–DiDomenico model. Experimental verification of Eq.12 can be obtained by plotting $(n^2-1)^{-1}$ versus $(h\nu)^2$ as illustrated in Fig.8 for $Se_{70}Ge_{30}$, which yields a straight line for normal behaviour having the slope $(E_o E_d)^{-1}$ and the intercept with the vertical axis equal to E_o / E_d. Values of E_o and E_d for $Se_{70}Ge_{30}$ thin films are 6.395 and 20.047eV, respectively. But the obtained curve in Fig. 8, shows a negative deviation from linearity. A negative curvature deviation at shorter wavelength is sometimes observed due to the proximity of the band edge or extonic absorption [20-21]. The values of E_o and E_d obtained by E. Márquez et al [19,22] are 4.88 and 21.81eV for $Ge_{0.25}Se_{0.75}$, 5.40 and 23.80eV for $Ge_{0.35}Se_{0.65}$, and 4.60 and 23.2eV for $GeSe_3$, respectively. The obtained values in this study are in good agreement with those obtained before. Furthermore, the dispersion energy follows a simple empirical relationship for covalent solid materials[20-21]:-

$$E_d = \beta N_c N_e Z_a\,, \tag{13}$$

where β is a constant, and according to Wemple [20-21], for covalent crystalline and amorphous materials has a value of 0.37±0.04 eV. N_c is the coordination number of the cation nearest neighbour to the anion, Z_a is the formal chemical valency of the anion and N_e is the effective

number of valence electrons per anion. In the present case, Z_a=2 [19]. Value of N_e was calculated according to the following equation [22]:

$$\mathrm{Ne} = \frac{((64x + 6(1-x))}{1-x} \quad , \quad x \neq 0 \tag{14}$$

The corresponding value of N_e for $Se_{70}Ge_{30}$ from the above equation equal 7.71. The obtained values of N_c according to Eq.13 equals 3.513 ($\beta = 0.37$).

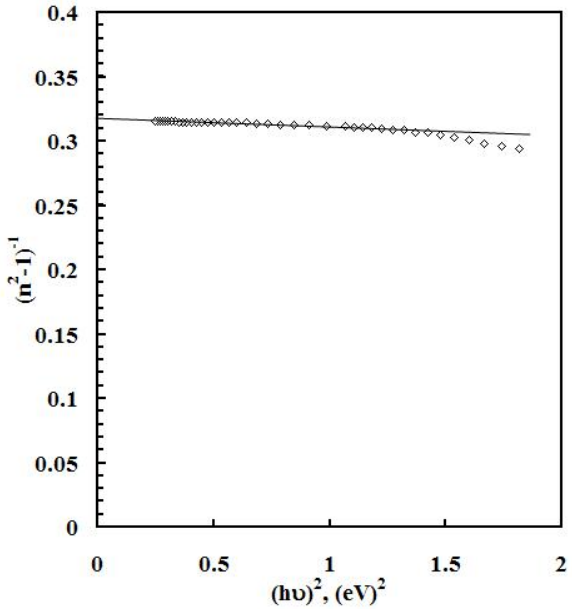

Fig. 8. Plots of $(n^2-1)^{-1}$ *against* $(h\nu)^2$ *for the investigated thin films.*

3.2.A. Determination of dielectric constants for $Se_{70}Ge_{30}$ thin films.

3.2.A.I. Determination of high frequency dielectric constant.

The obtained data of refractive index n can be analyzed to obtain the high frequency dielectric constant via two procedures [23]: the first procedure describes the contribution of the free carriers and the lattice vibration modes of the dispersion. The second procedure, however, is based upon the dispersion arising from the bound carriers in an empty lattice. To obtain a reliable value for the high frequency dielectric constant ε_∞, we employed both procedures.

(i) The first procedure:

The following equation can be used to obtain the high frequency dielectric constant [23]:

$$\varepsilon_1 = \varepsilon_{\infty(1)} - B\lambda^2 , \tag{15}$$

where

$$B = \frac{e^2 N}{4\pi^2 c^2 \varepsilon_o m^*} \tag{16}$$

where ε_1 is the real part of dielectric constant, $\varepsilon_{\infty(1)}$ the lattice dielectric constant or (the high frequency dielectric constant) according to first procedure, λ the wavelength, N the free charge carrier concentration, ε_o the permittivity of free space (8.854×10^{-12}F/m), m^* the effective mass of the charge carrier and c the velocity of light. The real part of dielectric constants $\varepsilon_1 = n^2$ was calculated at different values of λ. Then, the obtained values of ε_1 are plotted as a function *of* λ^2 as shown in Fig.9. It is observed that the dependence of ε_1 on λ^2 is linear at longer wavelengths. Extrapolating the linear part of this dependence to zero wavelength gives the value of $\varepsilon_{\infty(1)}$ and from the slopes of these lines, value of N/m^* for the investigated sample was calculated according to the Eq.16 of the constant B. The obtained values of $\varepsilon_{\infty(1)}$ and N/m^* are given in Table 2.

(ii) The second procedure:

The dielectric constant of a material could be calculated using the dispersion relation of incident photon. The refractive index was also fitted using a function for extrapolation towards shorter wavelengths. The model of Moss [24], which stated that the free carriers contribution to dispersion are relatively small. This means that data corresponding to the wavelength range lying below the absorption edge of the material are to be used. In such a case, one can apply the next relation. The properties of the investigated sample could be treated as a single oscillator at wavelength λ_o at high frequency. The high frequency dielectric constant can be calculated by applying the following simple classical dispersion relation [23]:

$$\frac{(n_o^2 - 1)}{(n^2 - 1)} = 1 - \left(\frac{\lambda_o}{\lambda}\right)^2, \tag{17}$$

where n_o is the refractive index at infinite wavelength λ_o (average interband oscillator wavelength), n the refractive index and λ the wavelength of the incident photon. Plotting $(n^2-1)^{-1}$ against λ^{-2} which showed linear part, was below the absorption edge as shown in Fig.10. The intersection with $(n^2-1)^{-1}$ axis is $(n_o^2-1)^{-1}$ and hence, n_0^2 at λ_o equal to $\varepsilon_{\infty(2)}$ (high frequency dielectric constant). Values of $\varepsilon_{\infty(2)}$ for $Se_{70}Ge_{30}$ thin films are given in Table.2. Eq.17 can also be written as [25]:-

$$(n^2 - 1) = \left(\frac{S_o \lambda_o^2}{1 - (\lambda^2/\lambda_o^2)}\right), \tag{18}$$

where S_o is the average oscillator strength which equals to:-

$$S_0 = \frac{(n_o^2 - 1)}{\lambda_o^2}, \tag{19}$$

Table.2. Values of $\varepsilon_\infty(1)$, $\varepsilon_\infty(2)$, λ_o, S_o and N/m^* for $Se_{70}Ge_{30}$ thin films.

Material	**From Fig. 9** $\varepsilon_{\infty(1)}$	**From Fig. 10** $\varepsilon_{\infty(2)}$	λ_o, **nm**	S_o, **m^{-2}**	N/m^*, **m^{-3}**
$Se_{70}Ge_{30}$	4.16	4.13	199.1	7.91×10^{13}	3.68×10^{54}

It is clear from Table.2 that the values of $\varepsilon_{\infty(1)}$ and $\varepsilon_{\infty(2)}$ obtained from the two procedures approximately agreed with each other, may be attributed to the lattice vibrations and bounded carriers in an empty lattice are in the transparent region [16]. The mean values of the high frequency dielectric constant for $Se_{70}Ge_{30}$ equal 4.146 ± 0.012.

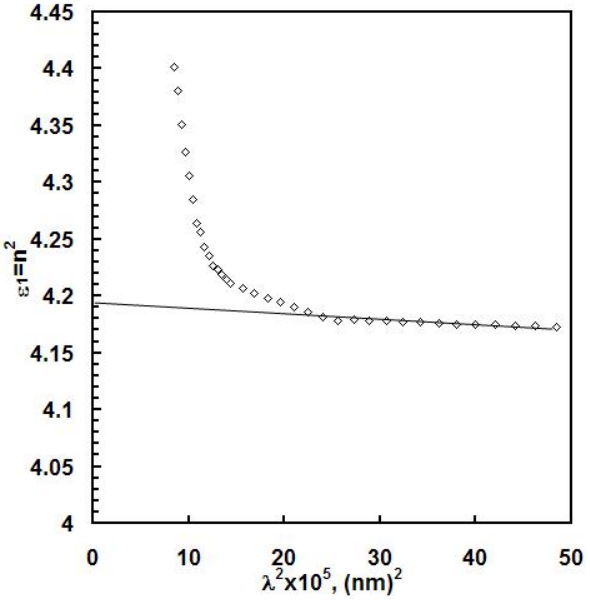

Fig. 9. Plots of ε_1 as a function of λ^2 for the investigated thin films.

3.2.A.II. Determination of complex dielectric constant.

The complex refractive index $\hat{n} = n + ik$ and dielectric function $\hat{\varepsilon} = \varepsilon_1 + i\varepsilon_2$ characterize the optical properties of any solid material. The imaginary and real parts of dielectric constant of thin films were also determined by the following relations [26-28]:

$$\varepsilon_1 = n^2 - k^2 = \varepsilon_\infty - \left(\frac{e^2 N}{4\pi^2 c^2 \varepsilon_o m^*}\right)\lambda^2 \tag{20}$$

and

$$\varepsilon_2 = 2nk = \left(\frac{\varepsilon_\infty \omega_p^2}{8\pi^2 c^3 \tau}\right)\lambda^3 , \tag{21}$$

where ε_1 is the real part, ε_2 the imaginary part of the dielectric constant, ε_∞ is the high frequency dielectric constant, ω_p is the plasma frequency, τ the optical relaxation time and

$k = \alpha\lambda / 4\pi$. the imaginary and real parts of the dielectric constant can be calculated as it is directly related to the density of states within the forbidden gap of the investigated sample [26-27]. The real and imaginary parts of the dielectric constant of the films are shown in Fig.11 for $Se_{70}Ge_{30}$ thin films. It is seen that both ε_1 and ε_2 increases with increasing photon energy. The real and imaginary parts follow the same pattern and it is seen that the values of real part are higher than the imaginary parts.

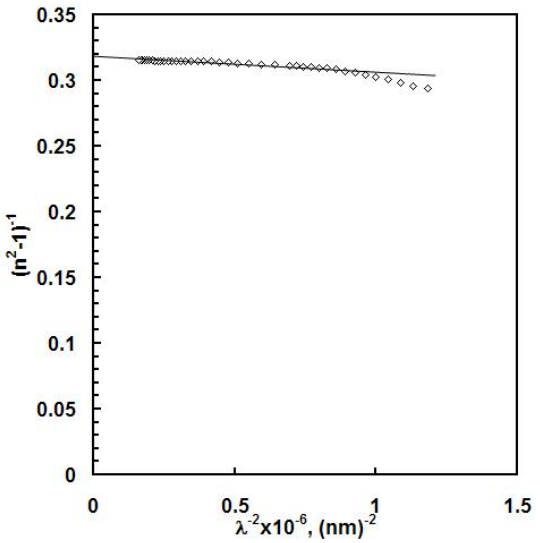

Fig.10. Plots of $(n^2 - 1)^{-1}$ *against* λ^{-2} *for the investigated thin films.*

For instance, the properties of a dielectric change on a time scale determined by the relaxation time when an external electric field is changed. This so-called dielectric relaxation time is a property of a solid that is closely related to its conductivity. The dielectric relaxation time is a measure of the time it takes for charge in a semiconductor to become neutralized by conduction process. it is small in metals and can be large in semiconductors and insulators. The dielectric relaxation time τ can be evaluated by using the relation [28-30]:

$$\tau = \frac{\varepsilon_\infty - \varepsilon_1}{\omega\varepsilon_2}, \tag{22}$$

Fig.12 depicts the dielectric relaxation time τ as a function of photon energy $h\nu$ for $Se_{70}Ge_{30}$ thin films. This figure showed that the relaxation time increases with increasing the photon energy.

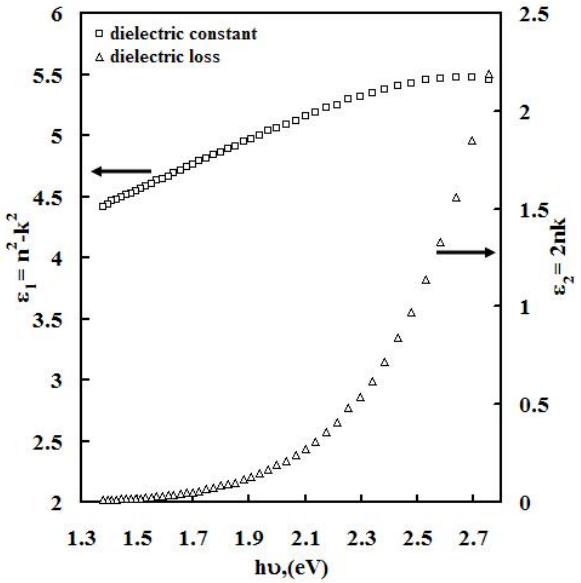

Fig.11 Plots of ε_1 and ε_2 as a function of $h\nu$ for the investigated thin films.

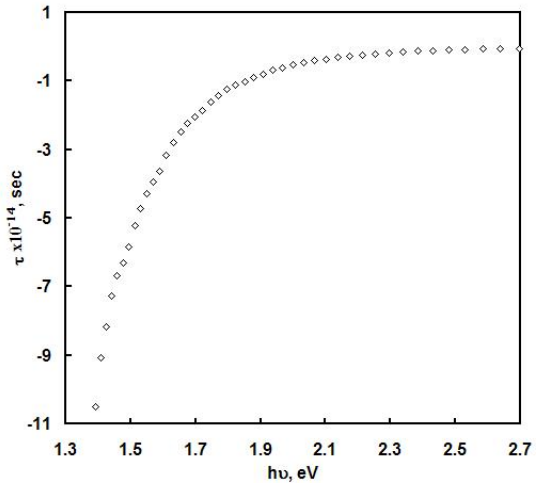

Fig.12 Dependence of the dielectric relaxation time τ on the photon energy $h\nu$ for the investigated thin films.

In physics, the dissipation factor (tanδ) is a measure of loss-rate of power of a mechanical mode, such as an oscillation, in a dissipative system. For example, electric power is lost in all dielectric materials, usually in the form of heat. The dissipation factor $\tan\delta$ can be calculated according to the following equation [25]:

$$\tan\delta = \frac{\varepsilon_2}{\varepsilon_1}, \tag{23}$$

The variation of dissipation factor of the investigated films with frequency υ is shown in Fig.13. It is found that the dissipation factor increases with increasing photon energy.

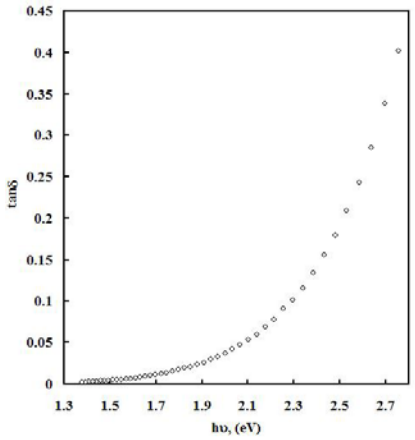

Fig.13 Dependence of dissipation factor $\tan\delta$ *on the photon energy* $h\nu$ *for the investigated thin films.*

The absorption coefficient α can be used to calculate the optical conductivity σ_{opt} as follow [31]:

$$\sigma_{opt} = \frac{\alpha nc}{4\pi}, \tag{24}$$

Fig.14 shows the variation of optical conductivity σ_{opt} as a function of photon energy $h\nu$. The increased of optical conductivity at high photon energies is due to the high absorbance of $Se_{70}Ge_{30}$ thin films and also may be due to the electron excited by photon energy [32].

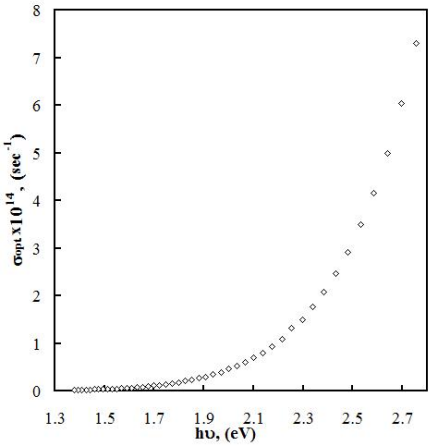

Fig.14 Dependence of optical conductivity σ_{opt} *on the photon energy* $h\nu$ *for the investigated thin films.*

4. Conclusions

The refractive index n and absorption index k were computed from the obtained $T(\lambda)$ using Swanepoel's method. On the basis of the optical investigations of the films, the following

results were obtained. The optical band gaps were calculated in terms of Tauc method and Wemple- DiDomenico model. The $E_{g(1)}^{opt}$ and $E_{g(2)}^{opt}$ are in agreement with each other and good agreement with the values obtained before. The type of optical transition responsible for optical absorption was indirect transitions. Values of the real part of the dielectric constant are higher than the imaginary part. The relaxation time τ, the dissipation factor $\tan\delta$ and the optical conductivity σ_{opt} were increased with increasing the photon energy.

References

[1] J. Feinleib, S. DeNeufville, C. Moss, S.R. Ovshinsky, Appl. Phys. Lett. **18,** 254 (1971).
[2] K.A. Rubin, M. Chen, Thin Solid Films **181**, 129 (1989).
[3] S.A. Khan, M. Zulfequar, M. Husain, Physica B **324**, 336 (2002).
[4] M.B. Elden, M.M. El-Nahass, Opt. Laser Technol., **35**, 335 (2003).
[5] Z.H. Khan, M. Zulfequar, Arvind Kumar, M. Husain, Con. J. Phys.**80**, 19 (2002).
[6] J. Nishi, S. Morimoto, I. Ingawa, R. Lizuka, T. Yamashita, J. Non-Cryst. Solids **140,** 199 (1992).
[7] G. Lucovsky, Phys. Rev. B, **15**, 5762 (1977).
[8] Burckhardt W, A. Feltz, Phys. Stat. Sol. (a) **80**, 463 (1983).
[9] M.A. Afifi, M. Fadel, E.G. El-Metwally, A.M. Shakra, Vacuum **77**, 259 (2005)–268.
[10] R. Swanepoel, J. Phys. E: Sci. Instrum., **16**, 1214 (1983).
[11] A.Y. İlker, Hüseyin Tolunay, Turk. J. Phy., **25**, 215 (2001).
[12] E.A. El-Sayes, G.B. Sakr, Phys. Stat. Sol. (a), **201**, 3060 (2004).
[13] H.T. El-Shair, Optica Pura Y Aplicda, **25**, 61 (1992).
[14] N. Kenny, C.R. Kannewurf, D.H. Whitmore, J. Phys. Chem. Solids **27**, 1237 (1966).
[15] N.F. Mott, E.A. Davis, Electronic Process in Non-Crystalline Materials, Calendron Press, Oxford, 1979.
[16] M.M. Abdel-Aziz, E.G. El-Metwally, M. Fadel, H.H. Labib and M.A. Afifi, Thin Solid Films, **386**, 99 (2001).
[17] J. Tauc, R. Grigorovici and A. Vancu, Phys. Status Solidi **15**, 627 (1966).
[18] N.A. Bakr, Journal of Materials Processing Technology, **132**, 138 (2003).
[19] J. Reyes, E. Márquez, J.B. Ramirez-Malo, C.Corrales, J. Fernández-Pena, P. Villares and R. Jiménez-Garay, Journal of Materials Science **30**, 4133 (1995).
[20] M. Didomenico and S.H. Wemple, J. Appl. Phys., **40**, 720 (1969).
[21] S.H. Wemple and M. Didomenico, Phys. Rev. B, **3**, 1338 (1971).
[22] E. Márquez, P. Nagels, J.M. González-Leal, A.M. Bernal-Oliva, E. Sleeckx, R. Callaerts, Vacuum **52**, 55 (1999).
[23] J.N. Zemel, J.D. Jensen, R.B. Schoolar, Phys. Rev. A, **140**, 330 (1965).
[24] T.S. Moss, Optical properties of semiconductors, London: Butter Worths Scientific Publication LTD, 1959.
[25] F. Yakuphanoglu, A. Cukurovali, I. Yilmaz, Physica B **351**, 53 (2004).
[26] A. El-Korashy, H. El-Zahed, M. Radwan, Physica B **334**, 75 (2003).
[27] M.M. Wakad, E.Kh. Shokr, S.H. Mohammed, J. Non-Cryst. Solids **265**, 157 (2000).
[28] M.M. Abdel-Aziz, I.S. Yahia, L.A. Wahab, M. Fadel, M.A. Afifi, Applied Surface Science **252**, 8163 (2006).
[29] R.J. Bell, M.A. Ordal, R.W. Alexender, Appl. Opt. **24**, 3680 (1985).
[30] M.Y. Han, H. Huang, C.H. Chew, L.M. Gan, X.J. Zhang, W. Ji, J. Phys. Chem. B **102**, 1884 (1998).
[31] J.I. Pankove, Optical processes in semiconductors, (Dover Publications, Inc. NewYork, 1975, p. 91.
[32] F. Yakuphanoglu, A. Cukurovali, I. Yilmaz, Optical Materials **27**, 1366 (2005).